Analysis of the Pantograph-Catenary Interaction in Railway Operations

José Mário Batista Rebelo
j.mario.rebelo@tecnico.ulisboa.pt
Instituto Superior Técnico, Universidade de Lisboa – Portugal
July 2019

Abstract: Railway is one the most worldwide spread and efficient transportation system for passengers and goods. In addition, electric traction railway vehicles present a safe, reliable and much needed alternative solution in a world where the need to reduce the use of fossil fuels and emission of greenhouse gases is critical. In this sense, making the railway operation as fast and efficient as possible is one of the key aspects to ensure railway competitiveness. One factor that has a significative impact on the overall performance of electric railway systems is its energy collection, achieved through the interaction between the train, via the pantograph, and the overhead electric line, known as catenary or overhead line. Ensuring the quality of this interface is essential to avoid contact losses, consequent electric arcing and electromechanical wear. Virtual testing, achieved via numeric simulation of the pantograph-catenary interaction, allows for easier, faster and less costly studies by reducing the need for on-site testing. This work, challenges the current standards for contact quality evaluation, presenting evidence on how long track lengths, curves, overpasses or contact wire height gradients, and dimensional defects may affect the standard dynamics analysis parameters. In addition, the developed studies address how train speed and the number and position of pantographs affects the contact force quality in the pantograph-catenary interaction. Several catenary models, based on the Network Rail Great Western Mainline catenary, are built, each with increasing complexity. Moreover, the interaction dynamics for each scenario is obtained, processed and analysed, in order to access how geometric singularities impact the performance of the pantograph-catenary interface.

Keywords: Railway Dynamics, Pantograph-Catenary Interaction, Curved track, Gradients, Geometric Defects.

1 Introduction

Railway systems are one of the major players in worldwide transportation of goods and passengers. Electric traction vehicles present a viable and much needed alternative in a world where there is a need to reduce the use of fossil fuels and emission of greenhouse gases. Despite being cost-effective, railways still require a considerable initial investment regarding infrastructure, track, vehicle and overhead lines, not only in economic terms but also in terms of planning, design and development. Shaping railway operations as efficiently as possible is one of the key aspects to ensure railways remain competitive against other means of transportation. Consequently, the reduction of operation and maintenance costs, in parallel with increasing operating speeds, is one of the main challenges the industry is facing. One factor that impacts operating speed limitations is the interaction between the train, via the pantograph, and the overhead electric line, known as catenary, in electrified railway lines.

The catenary is an overhead, current-carrying, structure composed by a set of wires and supporting elements with the task of supplying electricity to the train engines. The pantograph, a mechanism mounted on top of the railway vehicle, collects the electric current carried by the catenary via sliding contact between the catenary contact wire and the pantographs contact strips. The ability to maintain this contact uninterrupted is paramount to ensure sufficient power delivery to the railway vehicles. Higher contact forces in this interface lead to operating conditions with higher mechanical wear, leading to higher frequency of maintenance interventions and risk of failure. Lower contact forces may cause contact losses, which lead to lower energy collection, limiting the ability to maintain higher speeds, and electric arcing with consequent electro-mechanical wear. Virtual testing, achieved via simulation of the pantograph-catenary interaction, allows for faster and cheaper studies, reducing the need for on-site testing. Computational tools capable of handling the dynamics of this interface are employed not only for certification and validation of new vehicles and infrastructures, under varying scenarios, but also to reach optimized designs and optimal operating conditions.

The development and application of computational methods capable of simulating the pantograph-catenary interaction is currently an active field of research. The problems addressed include optimisation of pantograph and catenary designs (Bruni et al., 2012; Gregori et al., 2017), critical catenary sections (Antunes et al., 2014; Harèll, Drugge, and Reijm, 2005; Mei et al., 2006), multiple pantograph operation (Bucca et al., 2012; Liu et al., 2016; Pombo and Antunes, 2013), influence of aerodynamics effects, vehicle vibration and catenary irregularities (Carnicero et al., 2012; Pombo et al., 2009; Van et al., 2014) as well as identification and influence of catenary damping (Ambrósio, Antunes, et al., 2012; Nåvik, Rønnquist, and Stichel, 2016). In addition to these effects, pantograph-catenary benchmarks demonstrate how existing state-of-the art numerical tools being developed deal with, in most cases, simulation of the pantograph-catenary interaction in straight tracks (Bruni et al., 2014; Facchinetti and Bruni, 2015). However, real railway tracks are not strictly straight and present curves with different radii, track cant and differences in track elevation. Therefore, with particular exceptions such as

PantoCat (Ambrósio et al., 2015), most present pantograph-catenary numerical analysis tools cannot fully simulate catenary models with realistic geometries. Here, *PantoCat* presents an unique feature to address numerical analysis of general catenary geometries in interaction with the pantograph, further detailed in (Antunes et al., 2019). The work developed here employs this computational tool and its numerical procedures to simulate various scenarios, in other to better understand contact quality evaluation standards.

The main objective of this work is to challenge the currently adopted scenarios for contact quality evaluation, showing how long track lengths, curves, overpasses or contact wire height gradients, and dimensional defects may affect the analysis results. In addition, these studies address how train speed and the number and position of pantographs affects the contact force quality in the pantograph-catenary interaction. Various catenary models, based on the Network Rail Great Western Mainline catenary, are built. They present increasing complexity, from a single 1.2 km catenary section up to a 8 km catenary model with multiple sections, with realistic geometry, gradients and geometric defects. A Brecknell-Willis HSX pantograph, modelled as a lumped mass pantograph with data obtained from Deutsche Bahn experimental facilities, is used in all simulations. The interaction dynamics for the various catenary models is obtained, processed and analysed.

2 Catenary Dynamic Analysis and Modelling

Railway catenaries are overhead, current-carrying structures with the purpose of supplying electricity to the trains running on tracks below them. In their simplest form, catenaries are composed by two wires, the messenger wire and contact wire, tensioned at the supports in the beginning and end of each catenary section. Along the length of a section, the wires are periodically mounted on poles, and supported at each one by cantilevers, as seen in Figure 2.1 (a). The contact wire is supported from above by cable elements, known as droppers, that hang from the messenger wire, and allow to control the contact wire sag and elasticity. To ensure contact continuity in the pantograph contact strip, some of the terminal spans of a section and initial spans of the following section are overlapped, in what is commonly referred to as an overlapping section, as depicted in Figure 2.1 (b).

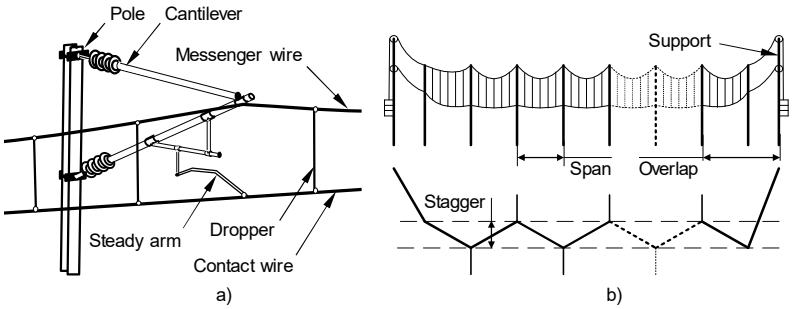

Figure 2.1: Catenary: (a) structural elements; (b) side and top views of a catenary section

To avoid excessive friction, heat and grooving of the pantograph contact strip, the contact wire is laterally displaced, due to the steady arms, so that it sweeps the contact strip as much as possible and distributes wear along its surface. This lateral offset is commonly known as stagger, as presented in Figure 2.1 b). The motion of the catenary system is characterized by small rotations and deformations, being well represented by linear finite element models. All catenary wires and structural components are modelled, in the finite element model, as a 2 node, 6 degree of freedom, Euler-Bernoulli beam element. An initialisation procedure, based on a minimisation problem, is employed to find the undeformed mesh of the catenary finite element system, such that when statically load it meets the correct geometrical shape given by the catenary data (Antunes, 2018). An implicit Newmark time integration algorithm, with a trapezoidal rule and constant time step, is used to solve the equations of motion. This particular method is chosen due to its unconditional stability nature when used implicitly and its proven robustness in finite element applications of the type demonstrated in this work (Antunes, 2018).

The GWML catenary model employed in this work is based on the British Network Rail Series 1 OLE system (Furrer+Frey, 2014). The data needed to model this catenary in straight track scenarios is available in the literature (BSI - EN 50318 2018).

3 Pantograph Dynamic Analysis and Modelling

Railway roof pantographs are systems with the aim to collect electric current from railway catenaries. These systems are designed so that the movement of the pantograph head is constrained to be in a straight line, perpendicular to the pantograph base. A series of jointed arms and links connect the pantograph head to the base. The pantograph contact strip, mounted on each of the pantograph bows, is responsible for the sliding contact with the catenary contact wire. Pantographs are mounted in perfect vertical alignment with the centre of the bogies of the vehicle, to ensure that the centre of the contact strip does not deviate from the centre of the track, even during banked corners. Pantograph models are required to behave realistically in the 0 – 20 Hz frequency range. Pantographs are commonly modelled using one of two representations: lumped-mass models and multibody models. Lumped-mass models present a simpler,

more commonly used approach to pantograph modelling. These systems are composed by a series of masses connected by springs, dampers and actuators. This methodology results in models such as the one depicted in Figure 3.1, generally with three mass-spring-damper stages. Unlike the multibody model, the parameters required to describe a lumped-mass model cannot be measured from physical characteristics of selected bodies of the real pantograph. Instead, the mass, spring and damper characteristics must be identified experimentally.

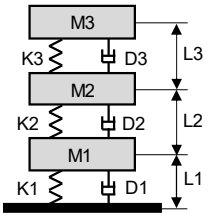

Stage	Masses $[kg]$	Dampers $[Ns/m]$	Springs $[N/m]$	Lengths $[m]$
1	3.53	32.6	0.000	0.20
2	7.50	0.00	5000	0.15
3	5.30	70.0	6300	0.10

Figure 3.1: Pantograph lumped-mass model

The lumped-mass models can be evaluated through a multibody formulation (Ambrósio et al., 2015). A multibody model is generically defined as a collection of bodies, whose motion is constrained by joints and acted on by external forces. The pantograph used in this computational work is the Brecknell-Willis British Rail HSX Pantograph, modelled as a 3-mass multibody system, according to the parameters identified by DB, in Munich. The car height is assumed to be 4.05 m, for a catenary contact wire nominal height of 4.7 m. Its modelling parameters are presented in Figure 3.1. An uplift force $\mathbf{f}_{up}$, with an intensity dependent on the targeted operation velocity of the pantograph, is applied upwards in mass M_1, to ensure that the mean contact force $\mathbf{f}_c$ in the pantograph-catenary interface fulfils that specified for the railway line maximum operational speed $\mathbf{v}$. According to standard EN50367:2012 (CENELEC - EN 50367, 2012), there is a maximum mean value of $\mathbf{f}_c$ $[N]$ to be enforced in each simulation scenario, given by:

$$\mathbf{f}_{c,max} = \begin{cases} 0.00047\mathbf{v}^2 + 90 & , \ \mathbf{v} \leq 200 \ km/h \\ 0.00097\mathbf{v}^2 + 70 & , \ \mathbf{v} \geq 200 \ km/h \end{cases} \quad [N] \tag{3.1}$$

4 Identification of Modelling Features for Realistic Catenary Modelling

The objective of this work is to evaluate how overlaps, curves, gradients and geometric defects affect the results of pantograph-catenary dynamics when operating at conventional speeds, in comparison with the usual straight track scenarios. The scenarios selected include the catenary of the Great Western Mainline (GWML). Simulations are carried for six different scenarios: single straight section, two straight sections with overlap, seven straight sections with overlap, and seven sections with realistic track geometry with and without gradients and geometric catenary defects. All scenarios are simulated with the same pantograph model, but for single and multiple pantograph operations at five different speeds.

4.1 Track Geometry

The full track geometry for simulation scenarios with realistic track is described in Table 4.1. The track curvature versus track length profile and the track length covered by each section are shown in Figure 4.1, where darker shades of grey represent overlapping zones. Sections 1 through 6 have twenty three 55-metre spans, resulting in a total section length of 1265 metres, and a total track length of 7975 metres.

Table 4.1: Track geometry for realistic scenarios

Zone	Zone length (m)	P_{km} (m)	R (m)	c (m^{-1})	Cant (mm)
		0.00	0.00	0.00000	0.00
Straight Track	1497.40	1497.40	0.00	0.00000	0.00
Transition Curve	445.20	1942.60	2400.00	0.00042	-150.00
Circular Curve	182.20	2124.80	2400.00	0.00042	-150.00
Transition Curve	445.20	2570.00	0.00	0.00000	0.00
Straight Track	150.70	2720.70	0.00	0.00000	0.00
Transition Curve	227.30	2948.00	-4700.00	0.00021	127.32
Circular Curve	2742.10	5690.10	-4700.00	0.00021	127.32
Transition Curve	227.30	5917.40	0.00	0.00000	0.00
Straight Track	2082.60	8000.00	0.00	0.00000	0.00

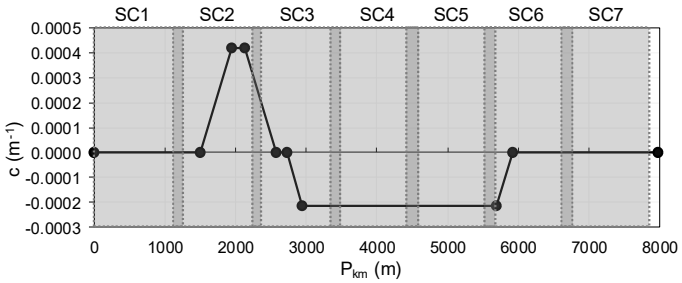

Figure 4.1: Track geometry for realistic scenarios and overall section disposition

4.2 Stagger in Curves

The stagger in the contact wire is designed to ensure wear is distributed through all the pantograph contact strip and avoid grooving. In addition, it also takes into account the span length, which should be set as long as possible to reduce costs .In a straight track the stagger usually takes the form of $b_{i+1} = -b_i$, as depicted in Figure 4.2 (a). i.e. alternating lateral deviations from the centre line. However, as the track curvature increases, the offset in the inner side of the curve is decreased, in order to keep the contact wire sweep inside the limits enforced by the operation safety conditions. In the case of low radius curves it may happen that the offset in the inner side is increased to the point of $b_{i+1} = b_i$, as seen in Figure 4.2 (c). Eventually, there is a point when constant inner stagger is not enough to meet operational requirements such as gauging and minimal rate of sweep. In these cases the length of the spans is shortened (Antunes et al., 2019; Kiessling et al., 2018).

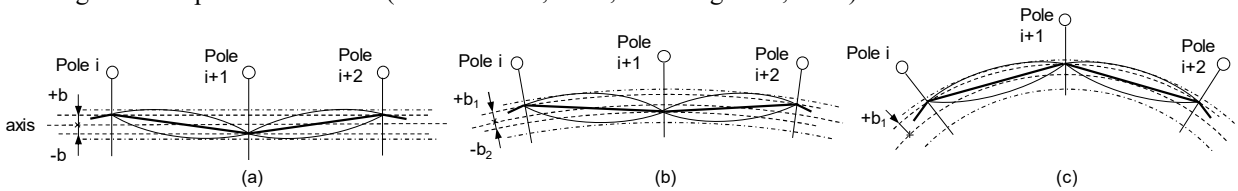

Figure 4.2: Contact wire stagger: (a) straight track; (b) large radius curves; (c) low radius curves

In the applications developed in this work, the stagger data for curved track for the GWM catenary is not available, and therefore, the design rules available and the best engineering judgment is used to build a stagger table for this catenary. When designing overhead contact lines, the rules for the stagger b at the registration arms are (Kiessling et al., 2018):

- Span length as long as possible;
- Contact wire sweep Δb_m > 1.5 mm/m;
- Contact wire sweep Δb_m < 1.5 mm/m is allowed for up to 30% of the span length;
- Lateral (radial) force at the supports 80 N < F_{lat} < 2000 N;
- Difference of lateral forces at adjacent supports as low as possible;

The pantograph contact wire sweep can be defined as the derivative of contact wire position in relation to the track centreline. The contact wire position in relation to the track centreline, $\mathbf{e}_{CW}$, expressed in mm, for span j, supported at poles i and $i-1$, is defined in the literature (Kiessling et al. 2018). The sweep Δb_m, in mm/m, is defined as:

$$\Delta b_m = \frac{d\mathbf{e}_{CW}}{d\mathbf{x}} = \frac{b_i - b_{i-1}}{L_j} + \frac{L_j - 2\mathbf{x}}{2R} \tag{4.1}$$

where b is the stagger in metres, L_j is the span length in metres, R is the curve radius in metres, and $\mathbf{x}$ is the position along the track in metres. The lateral forces in the steady arm at poles i and $i+1$, are given by (Kiessling et al. 2018):

$$F_{lat} = H\left(\frac{L_j}{R} + 2\frac{b_{i+1} \pm b_i}{L_j}\right) \tag{4.2}$$

where H is the contact wire tension expressed in N, and assuming that the stagger is constant at every other pole, this is, $b_{i+2} = b_i$.

By iteration and tuning, and using the guidelines explained above, a compromise between radius ranges, span lengths and staggers is achieved for the GWM catenary. This results in a stagger table for this particular catenary, which is presented in Table 4.2.

Table 4.2: Stagger data, lateral forces and rate of pantograph sweep for the GWM catenary

						MAX RADIUS					MIN RADIUS				
R (m)		Span	b1	b2	Tension	F_lat (N)	F_lat (N)	Δb (mm/m)			F_lat (N)	F_lat (N)	Δb (mm/m)		
<=	>	(m)	(mm)	(mm)	(N)	i	i+1	min	max	%bad_s	i	i+1	min	max	%bad_s
∞	15000	63	230	-230	16500	240.95	-240.95	7.30	7.30	0.00	310.25	-171.65	5.20	9.40	0.00
15000	7500	63	240	-230	16500	315.49	-176.89	5.36	9.56	0.00	384.79	-107.59	3.26	11.66	0.00
7500	6000	63	260	-230	16500	395.27	-118.07	3.58	11.98	0.00	429.92	-83.42	2.53	13.03	0.00
6000	5000	63	320	-230	16500	461.35	-114.85	3.48	13.98	0.00	496.00	-80.20	2.43	15.03	0.00
5000	4000	63	320	160	16500	291.71	124.09	0.00	8.84	23.81	343.68	176.07	0.00	10.41	19.05
4000	3300	63	320	190	16500	327.97	191.78	0.00	9.94	19.05	383.10	246.90	0.00	11.61	15.71
3300	2800	63	320	220	16500	367.38	262.62	0.00	11.13	15.71	423.63	318.87	0.00	12.84	13.33
2800	2500	63	320	250	16500	407.92	334.58	0.00	12.36	13.33	452.47	379.13	0.00	13.71	11.90
2500	2250	63	320	280	16500	436.75	394.85	0.00	13.23	11.90	482.95	441.05	0.00	14.63	10.71
2250	2000	63	320	320	16500	462.00	462.00	0.00	14.00	10.71	519.75	519.75	0.00	15.75	9.52

4.3 System Height Reduction

Along the track structures such as bridges pose geometric constraints to the catenary installation. These obstacles limit the free selection of pole positions and greatly limit the wiring geometry, often requiring height reduction of the entire catenary geometry. Minimum electrical and physical clearances between the each of the various current-carrying wires, the rails and the top of the overhead structure, are required to be met (CENELEC - EN 50119 2013).

The height reduction required to overcome the overhead obstacles can be achieved by following three processes, in which there is a priority on the process selected. This is, the next procedure is only attempted if the previous one does not allow for sufficient height reduction. The first procedure is to increase the midspan messenger wire sag by extending the span length to the maximum allowed in the area. The second procedure is to reduce the system height, i.e. messenger wire encumbrance at the supports, by reducing the dropper length down to the minimum acceptable values. The third procedure is to reduce the contact wire height, which must occur gradually, over the course of a number of gradient spans. This is to ensure contact continuity between the registration strip of the pantograph and the contact wire.

The data for the scenario under analysis in this work is bounded by the values described by the literature (Furrer+Frey, 2014). The regular span length is 55 m, the maximum design span length is 63 m, the minimum dropper length is 500 mm, the regular contact wire nominal height is 4.700 m and the minimum contact wire nominal height under bridges is 4.190 m. For speeds of 225 km/h, the maximum contact wire gradient is 1:1000 (1 ‰) and maximum gradient change between consecutive spans is 1:2000 (0.5 ‰). As the data for the real bridge over the railway track being studied is unavailable, the worst-case scenario is considered here. The overall gradient span arrangement for half of the gradient zone (GZ) can be seen in Figure 4.3, and the span description for half of the GZ can be seen in Table 4.3. There are gradients applied in section 4 and section 7 of the realistic track geometry, and the overall span arrangement of the sections mentioned is described in Table 4.4 and Table 4.5, respectively.

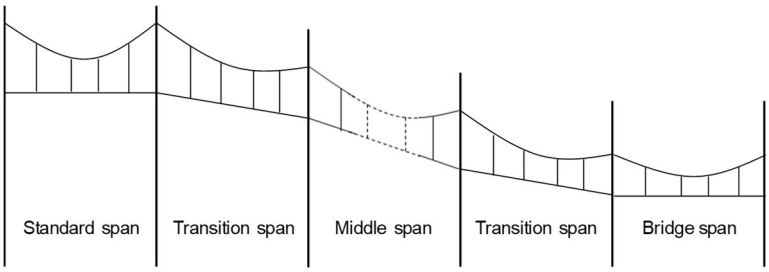

Figure 4.3: General geometry of a gradient zone (GZ); not all middle spans are shown; GZ is symmetrical at the bridge span

Table 4.3: Gradient zone (GZ) definition (only half the zone is shown)

Span number		1	2	3	4	5	6	7	8	9
Span type		1TR05	1TR1	2TR1	3TR1	4TR1	5TR1	6TR1	2TR05	BRIDGE
Span length (m)		55	55	55	55	55	55	55	55	63
Span gradient (‰)		-0.50	-1.00	-1.00	-1.00	-1.00	-1.00	-1.00	-0.50	0.00
CW height (m)	4.700	4.673	4.618	4.563	4.508	4.453	4.398	4.343	4.315	4.315
Gradient change (‰)	0.00	-0.50	0.00	0.00	0.00	0.00	0.00	0.50	0.50	0.00
Support number	1	2	3	4	5	6	7	8	9	10

Table 4.4: Section 4 overall span definition

Span number		1	2	3	4 - 11	12	13 - 20	21	22	23
Span type		AC55	OL55	FF55	GZ	BRIDGE	GZ	FF55	OL55	AC55
Span length (m)		55	55	55	55	63	55	55	55	55
CW height (m)	4.700	4.700	4.700	4.700	4.315	4.315	4.700	4.700	4.700	4.700
Support number	1	2	3	4	12	13	21	22	23	24

Table 4.5: Section 7 overall span definition

Span number		1	2	3	4 - 11	12	13 - 20	21	22	23	24	25
Span type		AC55	OL55	FF55	GZ	BRIDGE	GZ	FF55	FF55	FF55	OL55	AC55
Span length (m)		55	55	55	55	63	55	55	55	55	55	55
CW height (m)	4.700	4.700	4.700	4.700	4.315	4.315	4.700	4.700	4.700	4.700	4.700	4.700
Support number	1	2	3	4	12	13	21	22	23	24	25	26

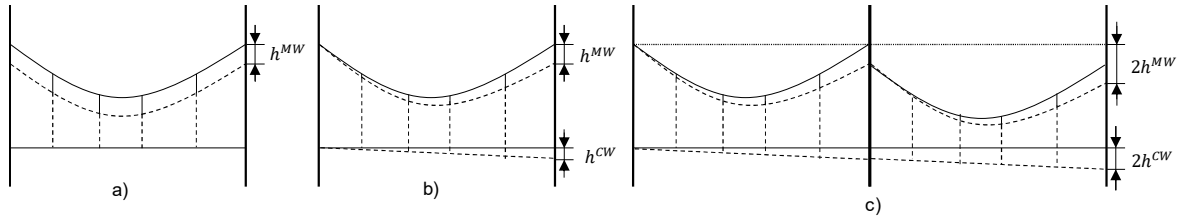

Figure 4.4: Height reduction: (a) constant system height (SH) reduction; (b) SH and CW height reduction in gradient spans; (c) Propagating effect of gradient affected height reduction

The system height and contact wire height reduction in a span is affected not only by its own gradient, but also by the gradients of the previous spans, as shown in Figure 4.4 (c). The dropper arrangement of the gradient spans was numerical evaluated for the span types detailed in Table 4.3. The length of dropper i in span j will be:

$$l_i = FF55_i + h_{r,1‰}\left[\left(\sum_1^{j-1} g_j\right) + g_j \frac{p_i}{L_j}\right] \tag{4.3}$$

where $FF55_i$ is the length of dropper i in the standard FF55 span, $h_{r,1‰}$ is the height reduction per 1‰ gradient span, g_j is the gradient applied to span j, p_i is the horizontal position of dropper i in its span, and L_j is the total length of span j. Pre-sag is considered, with maximum sag of 1‰.

4.4 Geometric Dimensional Defects

Catenary models generally consider the nominal dimensions of the various catenary structures. However, catenary installations exhibit geometric variations from the nominal values as time passes, as a result of the pantograph-catenary interaction, weather or infrastructure modifications. Infrastructure managers set tolerances on the catenary geometric parameters to decide whether the catenary needs maintenance, or if the dimensional defects do not affect railway operation and, therefore, do not require intervention. The combination of these dimensional variations throughout the catenary wires are acceptable if they remain under the specified tolerances. It may be argued that the defect distribution is not purely random but follows a dispersion around a set of specified wave lengths. However, as there is no data available regarding this issue, the application of random defects on the parameters that describe catenary geometry and pantograph base kinematics is used here as a way to model such deviations. Tolerance values for the selected parameters, obtained from the literature, are summarized in Table 4.6 (Furrer+Frey 2014; Kiessling et al. 2018).

Table 4.6: Tolerances for selected catenary parameters

CW height [mm]	± 15, open route ± 10, bridge areas
CW stagger [mm]	± 30

The method selected to generate the random numbers is the *rand()* function in *MatLab*, which uses the Mersenne Twister pseudorandom number generator (Matsumoto and Nishimura 1998). The geometry of the contact wire with height and stagger defects for selected sections of scenario S5 can be seen in Figure 4.5 and Figure 4.6, respectively.

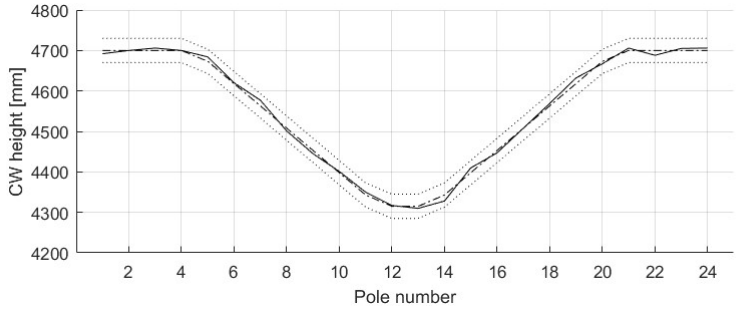

Figure 4.5: Contact wire height for section SC4 of scenario S6

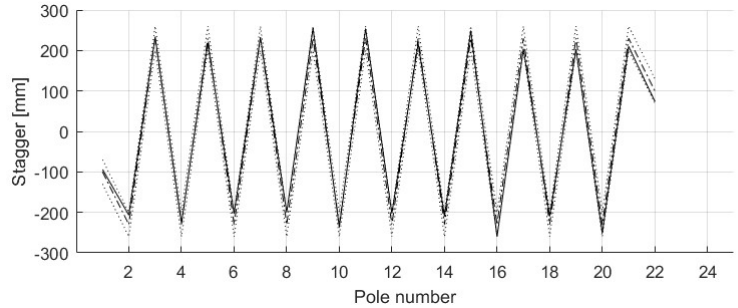

Figure 4.6: Contact wire stagger for section SC1 of scenario S6

5 Simulation Cases

The objective of this work is to evaluate how realistic catenary geometries, i.e. catenaries including overlaps, curves, gradients and defects, affect the results of pantograph-catenary simulation at conventional speeds, compared to the usual straight track scenarios. Scenarios 1, 2 and 3 include only straight tracks, despite their varying length, while scenarios 4, 5 and 6 use the realistic track geometry, shown in Figure 4.1. To fully evaluate how each degree of complexity on the catenary model affects the contact quality, a matrix of simulations is built, as seen in Table 5.1. In this table, **1**, **2** or **1,2** denotes instances where simulations are evaluated with a single pantograph, two pantographs, or both. Scenario S3 is used purely as a benchmark for simulations with a large number of sections. This level of complexity, in what the catenary model here considered is concerned, is not reported in the literature. Likewise, scenario S6 with a single pantograph is not simulated, as its behaviour is similar to that of the leading pantograph in a two-pantograph scenario. For each simulation the contact force results are evaluated for a set of zones of interest: the complete catenary and for each individual section. The contact force results are analysed only for the trailing pantograph, as it is the pantograph that shows worst contact performance.

Table 5.1: Simulation matrix for one pantograph operation

		SCENARIO					
		S1	S2	S3	S4	S5	S6
		Straight 1 section	Straight 2 sections	Straight 7 sections	Realistic	Realistic w/ gradients	Realistic w/ gradients and defects
SPEED (% of max catenary speed)	50%	1,2	1,2	-	1,2	1,2	2
	75%	1,2	1,2	-	1,2	1,2	2
	90%	1,2	1,2	-	1,2	1,2	2
	100%	1,2	1,2	1	1,2	1,2	2
	110%	1,2	1,2	-	1,2	1,2	2

The uplift force to be applied to the pantograph varies with the speed at which the pantograph runs. This and other simulation specific parameters are described in Table 5.2. For simulations carried with two pantographs the leading pantograph is placed at 218.25 m from the start of the catenary, this is, 100 m in front of the trailing pantograph.

Table 5.2: Simulation parameters

Speed [%]	Speed $[km/h]$	$\mathbf{f}_{up}$ $[N]$	Panto start length $[m]$
110%	247.50	129.4186	118.25
100%	225.00	119.1063	118.25
90%	202.50	109.7761	118.25
75%	168.75	103.3840	118.25
50%	112.50	95.9484	118.25

Contact quality is evaluated through statistical measures of the catenary contact force between the contact wire and pantograph registration strip(s). The contact force results are filtered in the 0 – 20 Hz range, according to the applicable standards. The contact force results are shown as contact force histograms and in statistical parameter tables, which include the contact force maximum, minimum, amplitude, mean, standard deviation, statistical maximum and statistical minimum, in addition to percentage of contact loss. The verification of quality of current collection is achieved by assessing the contact force maximum, mean and standard deviation, as well as the percentage of contact loss. The limiting values for the mean contact force are the same as the uplift force values described in Table 5.2, which are computed using equation 6.1. Maximum contact force must not exceed 350 N. Standard deviation must not exceed 30% of the mean contact force. The percentage of contact loss must not exceed 0.1% for speeds up to 250 km/h, and 0.2% for speeds above 250 km/h (Bruni et al. 2014; CENELEC - EN 50367 2012).

5.1 Influence of curves in the catenary model

The scenario S4, based on the realistic track geometry with curves, is modelled, using the data shown in the previous sections, and its simulation results compared to those obtained for scenario S2. A comparison for the trailing pantograph, running at 100% and 110% speeds in these scenarios, is shown in Figure 5.1. It can be seen that the contact performance deteriorates for the scenario with realistic geometry, especially for train speed of 100% of the catenary design speed. The maximum contact force increases and the minimum contact force decreases, which also leads to an increase in contact force amplitude. However, the maximum contact force for the trailing pantograph in scenario 2, i.e. two straight section with overlap, is much higher than that of the same pantograph, at the same speed, in the scenario with realistic geometry. Nevertheless, both values represent poor contact performance, as they are above the limit of 350 N.

	100% Speed		110% Speed	
	S2	S4	S2	S4
Maximum [N]	310.078	332.387	461.095	366.387
Minimum [N]	39.650	20.566	-11.463	-11.228
Amplitude [N]	270.428	311.821	472.558	377.615
Mean [N]	119.090	119.094	129.433	129.412
Standard Deviation [N]	26.986	29.580	41.918	30.140
Statistical Maximum [N]	200.048	207.835	255.189	219.833
Statistical Minimum [N]	38.131	30.353	3.678	38.991
Contact Losses [%]	0.000	0.000	0.062	0.048

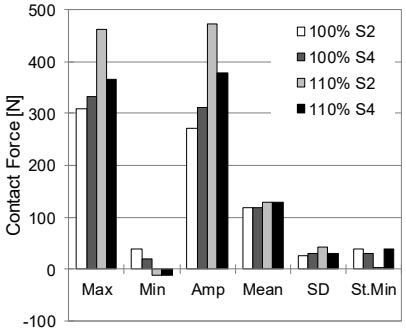

Figure 5.1: Results for trailing pantograph, running at various speeds in scenarios S2 and S4, all sections

5.2 Influence of gradients in the catenary geometry

In order to simulate the influence of contact wire gradients in the pantograph-catenary interaction a new scenario, based on scenario S4, is modelled. The track and catenary geometry remain the same, apart from sections 4 and 7 where the gradient zones are applied. Therefore, any variations in the contact force results, with respect to those obtained in scenario S4, are a consequence of the existence of gradient sections. The results for the trailing pantograph, running at 100% and 110% speed, are shown in Figure 5.2. It can be seen that the variations are minimal, which is to be expected if the gradient zones are well designed.

	100% Speed		110% Speed	
	S4	S5	S4	S5
Maximum [N]	332.387	337.615	366.387	356.688
Minimum [N]	20.566	12.237	-11.228	-2.791
Amplitude [N]	311.821	325.378	377.615	359.479
Mean [N]	119.094	119.096	129.412	129.415
Standard Deviation [N]	29.580	29.428	30.140	29.691
Statistical Maximum [N]	207.835	207.381	219.833	218.489
Statistical Minimum [N]	30.353	30.811	38.991	40.340
Contact Losses [%]	0.000	0.000	0.048	0.041

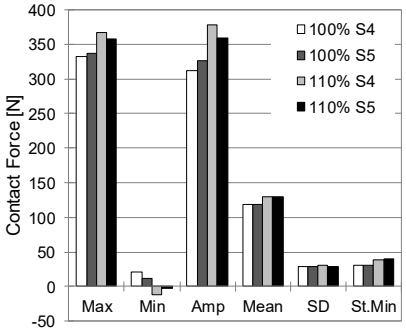

Figure 5.2: Results for trailing pantograph, running at various speeds in scenarios S4 and S5, all sections

5.3 Influence of geometry defects

In order to simulate the how dimensional defects in the contact wire height and stagger affect the pantograph-catenary interaction, a model is developed for a new scenario, based on scenario S5, with these defects applied. Any variations in the contact force results are associated to the catenary defects. The contact force results for the trailing pantograph, running at 100% and 110% speeds in the scenarios, are shown in Figure 5.3. It can be seen that for the trailing

pantograph at 110% speed the performance has a noticeable degradation, especially regarding the contact force maximum, amplitude and percentage of contact loss. The increasing catenary complexity also impacts the contact force distribution, which progressively approaches a shape closer to that of a normal distribution, as seen in Figure 5.4. SK and EK represent the skewness and excess kurtosis of the contact force distributions, respectively.

	100% Speed		110% Speed	
	S5	S6	S5	S6
Maximum [N]	337.615	333.360	356.688	404.963
Minimum [N]	12.237	22.864	-2.791	-14.256
Amplitude [N]	325.378	310.495	359.479	419.219
Mean [N]	119.096	119.094	129.415	129.414
Standard Deviation [N]	29.428	29.600	29.691	30.339
Statistical Maximum [N]	207.381	207.894	218.489	220.431
Statistical Minimum [N]	30.811	30.294	40.340	38.397
Contact Losses [%]	0.000	0.000	0.041	0.095

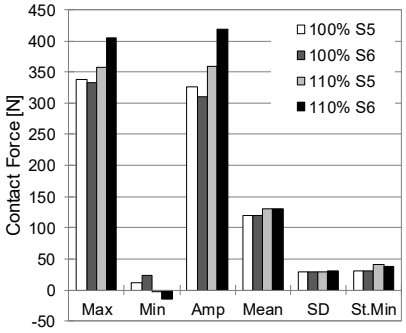

Figure 5.3: Results for trailing pantograph, running at various speeds in scenarios S5 and S6, all sections

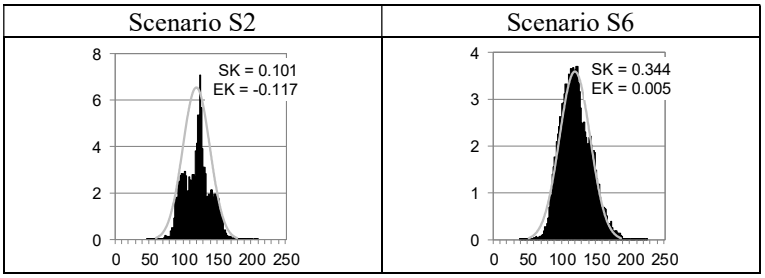

Figure 5.4: Force distribution for the leading pantograph, running at 100% speed in scenario S2 and S6, all sections

6 Conclusions and Future Work

In this work, six catenary models are developed, from a catenary with a single section in straight line, up to a catenary with 7 sections, 8 km of total length, with realistic geometry, gradients and geometric defects applied. The interaction between the train pantograph and the contact wire of the catenary for each scenario is simulated for five different speeds, in operating conditions of a single and two pantographs, and the contact force results compared. For a pantograph separation of 100 m, the leading pantograph behaves in a similar manner to that of a single pantograph. However, the trailing pantograph is affected by the propagating wave generated by the leading pantograph, and its contact performance is greatly decreased. The trailing pantograph, under operating speed of 110% of the maximum allowed catenary speed, is the only one to present maximum contact forces above the specified limit of 350 N, and the occurrence of contact losses, even if they remain under the specified limit of 0.2% for all scenarios. Nevertheless, this shows that evaluating contact performance for a single pantograph cannot be extrapolated for operating conditions with two or more pantographs. Catenary models with longer track lengths, that include a realistic track geometry, promote larger variations in the pantograph-catenary interaction results. Most of the effects of the inclusion of track cant and track curvature are seen in the contact force distributions, which take a shape closer to that of a normal distribution as catenary complexity increases. This effect is further enhanced by the presence of catenary gradients and geometric catenary defects. Real train operation does not happen with perfectly nominal track, pantograph and catenary geometries, and the addition of these singularities to the catenary helps achieve a model that more accurately represents what occurs in a more realistic pantograph-catenary interaction.

The work here presented details how curves, gradients and geometric defects in the catenary impact the pantograph-catenary interaction. However, most of the data required to model these singularities is not publicly available, and well justified workarounds are used, such as reconstructing the track geometric information from aerial images and track design handbooks, and building stagger tables using the limits for lateral steady arm forces and pantograph sweep available in the literature. Models built using actual track and catenary data, provided by the infrastructure owners, can take the work here developed even further, by comparing the simulation results of accurately built models with actual track line measurements. Likewise, data concerning the pantograph bodies can be used to build full multibody pantograph models, which allow for the insertion of pantograph irregularities.

The catenary geometric defects used in the work here present, at the lack of further information, are based on a random distribution of numbers lower than the tolerances specified by the infrastructure owners. Future in line tests and measurements may be performed to find more data regarding the propagation of defects in catenary wires and track rails, due to train operation. Even if these defects stay below the specified tolerances, their joint effect causes a degradation of contact quality between the pantograph and catenary that can be further analysed.

7 References

Ambrósio, J et al. 2012. “A Computational Procedure for the Dynamic Analysis of the Catenary-Pantograph Interaction in High-Speed Trains.” *Journal of Theoretical and Applied Mechanics* 50(3): 681–99.

Ambrósio, J, J Pombo, P Antunes, and M Pereira. 2015. “PantoCat Statement of Method.” *Vehicle System Dynamics* 53(3).

Ambrósio, J, J Pombo, P Antunes, and M Pereira. 2015. “PantoCat Statement of Method.” *Vehicle System Dynamics* 53(3): 314–28. http://www.tandfonline.com/doi/full/10.1080/00423114.2014.969283#.Vb-jZK2b2Hs.

Antunes, P. 2018. “Co-Simulation Methods for Multidisciplinary Problems in Railway Dynamics.”

Antunes, P, J Ambrósio, J Pombo, and A Facchinetti. 2019. “A New Methodology to Study the Pantograph – Catenary Dynamics in Curved Railway Tracks.” *Vehicle System Dynamics* 3114. https://doi.org/10.1080/00423114.2019.1583348.

Antunes, P, J Ambrósio, J Pombo, and M Pereira. 2014. “Dynamic Analysis of the Pantograph-Catenary Interaction on Overlap Sections for High-Speed Railway Operations.” In *Proceedings of the Second International Conference on Railway Technology: Research, Development and Maintenance*, Stirlingshire, UK: Civil-Comp Press. http://www.ctresources.info/ccp/paper.html?id=7792.

Bruni, S et al. 2014. “The Results of the Pantograph–Catenary Interaction Benchmark.” *Vehicle System Dynamics* 53(3): 412–35. http://www.tandfonline.com/doi/full/10.1080/00423114.2014.953183#abstract.

Bruni, S, G Bucca, A Collina, and A Facchinetti. 2012. “Numerical and Hardware-In-the-Loop Tools for the Design of Very High Speed Pantograph-Catenary Systems.” *Journal of Computational and Nonlinear Dynamics* 7(4): 41013. http://computationalnonlinear.asmedigitalcollection.asme.org/article.aspx?articleid=1475931.

BSI. 2018. “BS EN 50318 : Railway Applications - Current Collection Systems - Validation of Simulation of the Dynamic Interaction between Pantograph and Overhead Contact Line.” 3: 90.

Bucca, G et al. 2012. “Adoption of Different Pantographs Preloads to Improve Multiple Collection and Speed up Existing Lines.” *Vehicle System Dynamics* 50(SUPPL. 1): 403–18.

Carnicero, A et al. 2012. “Influence of Track Irregularities in the Catenary-Pantograph Dynamic Interaction.” *Journal of Computational and Nonlinear Dynamics* 7(4): 41015. http://computationalnonlinear.asmedigitalcollection.asme.org/article.aspx?articleid=1475933.

CENELEC - EN 50119. 2013. “Railway Applications. Fixed Installations. Electric Traction Overhead Contact Lines.”

CENELEC - EN 50367. 2012. “Railway Applications - Current Collection Systems - Technical Criteria for the Interaction between Pantograph and Overhead Line.”

Facchinetti, A, and S Bruni. 2015. “Special Issue on the Pantograph-Catenary Interaction Benchmark.” *Vehicle System Dynamics* 53(3): 303–4.

Furrer+Frey. 2014. *MAN001 System Description Manual*.

Gregori, S, M Tur, E Nadal, and F J Fuenmayor. 2017. “An Approach to Geometric Optimisation of Railway Catenaries.” *Vehicle System Dynamics* 3114(December): 1–25. https://www.tandfonline.com/doi/full/10.1080/00423114.2017.1407434.

Harèll, P, L Drugge, and M Reijm. 2005. “Study of Critical Sections in Catenary Systems During Multiple Pantograph Operation.” *Proceedings of the Institution of Mechanical Engineers, Part F: Journal of Rail and Rapid Transit* 219(4): 203–11. http://pif.sagepub.com/lookup/doi/10.1243/095440905X8934.

Kiessling, F et al. 2018. *Contact Lines for Electric Railways: Planning, Design, Implementation, Maintenance*. 3rd ed. Publicis.

Liu, Z, P A Jönsson, S Stichel, and A Rønnquist. 2016. “Implications of the Operation of Multiple Pantographs on the Soft Catenary Systems in Sweden.” *Proceedings of the Institution of Mechanical Engineers, Part F: Journal of Rail and Rapid Transit* 230(3): 971–83.

Matsumoto, M, and T Nishimura. 1998. “Mersenne Twister : A 623-Dimensionally Equidistributed Uniform Pseudorandom Number Generator.”

Mei, G, W Zhang, H Zhao, and L Zhang. 2006. “A Hybrid Method to Simulate the Interaction of Pantograph and Catenary on Overlap Span.” *Vehicle System Dynamics* 44(S1): 571--580.

Nåvik, Pr, A Rønnquist, and S Stichel. 2016. “Identification of System Damping in Railway Catenary Wire Systems from Full-Scale Measurements.” *Engineering Structures* 113: 71–78.

Pombo, J et al. 2009. “Influence of the Aerodynamic Forces on the Pantograph-Catenary System for High Speed Trains.” *Vehicle System Dynamics* 47(11): 1327–47.

Pombo, J, and Pe Antunes. 2013. “A Comparative Study Between Two Pantographs In Multiple Pantograph High-Speed Operations.” *Internatinal Journal of Railway Technology* 2(1): 83–108.

Van, O V, J P Massat, C Laurent, and E Balmes. 2014. “Introduction of Variability into Pantograph-Catenary Dynamic Simulations.” *Vehicle System Dynamics* 52(10): 1254–69. https://doi.org/10.1080/00423114.2014.922199.